

A Simple Free-Flow Traffic Model for Vehicular Intermittently Connected Networks

Maurice J. Khabbaz, Wissam F. Fawaz, and Chadi M. Assi, *Senior Member, IEEE*

Abstract—The performance of vehicular data networks (VDNs) is highly dependent on vehicular traffic. Existing studies on VDNs consider custom-developed traffic models that mimic real-life vehicular traffic behavior and prepare the ground for accurate VDN performance evaluation. Traffic evolution is affected by numerous random events. Some developed models are microscopic. They independently consider some possible factors (e.g., weather, road geometry, and drivers' skills). These microscopic models are complex, and their implementations may be costly. Other models are macroscopic. They revolve around only the following three major traffic parameters: 1) density; 2) flow; and 3) speed. The majority of such existing models are unrealistic, because they are based on restrictive assumptions tailored to their enclosing study. Comparing the performance of VDN protocols becomes adequate if and only if these protocols are all developed on top of the same traffic model. Unfortunately, the opposite is true. Hence, the design of a generic traffic model that serves as a basis for future studies on VDNs is equally urgent and important. This paper presents a comprehensive and traffic-theory-inspired macroscopic description of vehicular traffic behavior over roadway facilities that operate under free-flow traffic conditions. Accordingly, a simple and tractable macroscopic traffic model is proposed. Extensive simulations are conducted to verify the validity of the proposed model and its high accuracy.

Index Terms—Free-flow, modeling, queueing, traffic, vehicular.

I. INTRODUCTION

THE CONCEPTION of vehicular data networks (VDNs) consists of transforming vehicles into intelligent mobile entities that can wirelessly communicate with each other and with stationary roadside units (SRUs). This way, a highly

dynamic self-organized network that supports a large variety of safety,¹ convenience, and leisure² applications can be formed.

Pragmatically, researchers, network operators and engineers, as well as the large vehicular industry and some government authorities, have shown a recent interest in this emerging networking conception [1]–[6]. In fact, the majority of the leading vehicle manufacturers are producing communication-enabled vehicles that are equipped with small yet powerful wireless devices, Global Positioning System (GPS) units, navigation systems that are loaded with digital maps, and a large number of real-time monitoring sensors. The U.S. Federal Communications Commission (FCC) has dedicated the 5.9-GHz band for short/medium-range communication services that support intelligent transportation systems to expedite intervehicle and vehicle-to-roadside communication [7]–[9].

As opposed to traditional wireless ad hoc networks [10], a vehicular network exhibits volatile connectivity and has to handle a variety of network densities. For example, a vehicular network that is deployed over a rural roadway or within an urban area is likely to experience higher nodal densities. This case is particularly true during rush hours (e.g., 8:00–10:00 A.M. and 4:00–7:00 P.M.). However, during late-night hours and whenever deployed over large highways or within scarcely populated areas, a vehicular network is expected to suffer from frequent network partitioning and repetitive link disruptions. Over the last couple of years, the networking research community has witnessed many publishable studies that revolve around the connectivity analysis and the proposal of routing and forwarding schemes that handle the broadcast storm (e.g., [11] and [12]) and data delivery (e.g., [13]) in the context of a dense vehicular network. These studies were conducted under the simplified assumption that these vehicular networks are naturally well connected. In contrast, although the development of reliable, timely, and resource-efficient forwarding schemes that support the diverse topologies of *vehicular intermittently connected networks* (VICNs) is crucially challenging, it is believed that the immature understanding of network disruption causes and resolution procedures persistently leads to inadequate scheme designs and inaccurate performance analysis and evaluation.

Manuscript received September 28, 2011; revised December 19, 2011; accepted February 1, 2012. This work was supported by a Natural Sciences and Engineering Research Council of Canada research discovery grant. The Associate Editor for this paper was M. Da Lio.

M. J. Khabbaz is with Concordia University, Montreal, QC H3G 1M8, Canada (e-mail: mkhabbaz@ece.concordia.ca).

W. F. Fawaz is with the Lebanese American University, Byblos, Lebanon (e-mail: wissam.fawaz@lau.edu.lb).

C. M. Assi is with the Concordia Institute for Information Systems Engineering, Concordia University, Montreal, QC H3G 1M8, Canada (e-mail: assi@ece.concordia.ca).

Color versions of one or more of the figures in this paper are available online at <http://ieeexplore.ieee.org>.

Digital Object Identifier 10.1109/TITS.2012.2188519

¹The propagation of warning messages, including but not limited to real-time traffic state (e.g., position, speed, and direction of surrounding vehicles) and environmental data (e.g., congestion, pollution degrees, roaming patterns, and driving habits), in an attempt to predict and alert drivers of possible critical situations.

²Applications that were designed to promote passenger and driver comfort (e.g., traffic-aware route recommendation, Internet access, file sharing, and peer-to-peer services).

Although the universally known delay-tolerant networking (DTN)/disruption-tolerant networking's *store-carry-forward* mechanism (see [14]) has emerged as a highly effective solution that mitigates VICNs' link disruptions, the published performance evaluations of various VICN forwarding schemes that adopt this mechanism have been shown to be inconsistent with real-life experimental observations. Since then, the networking research community has been expressing a growing interest in uncovering the major cause of this inconsistency. Recently, several researchers have linked and proved that the reason behind this conflict between the real-world experimental observations and the theoretical analysis is the utilization of unrealistic theoretical vehicular traffic models (for example, see [16] and [17]). Following this case, every published work enclosed a customized model that attempts to emulate the realistic behavior of vehicular traffic. The vehicular traffic is affected by a large number of random events (e.g., weather, road geometry, drivers' skills and habits, and haphazard catastrophic incidents). So far, the open literature lacks any model that accounts for all such events. However, some of the developed models tend to have a microscopic aspect (for example, see [18] and [19]), because they independently consider factors such as weather, road geometry, commuter's skills, and habits. These microscopic models are complex, which renders them highly theoretical with limited implementation feasibility for simulations. Other models take on the macroscopic aspect (for example, see [20] and [21]). Macroscopic models revolve around the following three major traffic parameters: 1) the vehicular density; 2) the traffic flow; and 3) vehicles' speeds. Most of the existing models deviate from reality, because they are based on highly restrictive assumptions (e.g., all vehicles navigate at a single constant speed, and vehicles' speeds are independent of the vehicular density) tailored to their enclosing study. Ultimately, because existing VICN forwarding schemes have different underlying traffic models, comparing their performance is not meaningful.

This paper aims at achieving the following three objectives:

- 1) To present a comprehensive and traffic-theory-inspired macroscopic description of free-flow traffic conditions, i.e., conditions³ where vehicular traffic is typically characterized by low to medium vehicular density, arbitrarily high mean speeds, and stable flow, over 1-D uninterrupted⁴ roadway segments, the purpose of which is to introduce a generic notation for the aforementioned three macroscopic traffic parameters and highlight the strong correlation between them;
- 2) To propose a novel and universal simple free-flow traffic model (SFTM) that is based on the presented free-flow traffic behavior description;
- 3) To conduct a case study with the purpose of giving more insight into the integration of the proposed SFTM traffic model into the design and analysis of VICN forwarding schemes.

³Note that, under such conditions, delay tolerance becomes a major requirement for successful data delivery, because low to medium vehicular density coupled with high vehicle speeds causes the network to become sparse and subject to frequent link disruptions.

⁴No grade intersections, traffic lights, stop signs, direct access to adjacent lands, and bifurcations.

The remainder of this paper is organized as follows. In Section II, a selection of major related work is discussed, along with the novel contributions enclosed in this paper. Section III presents a comprehensive description of the free-flow traffic model, based on which the novel SFTM is proposed. In Section IV, extensive simulations are conducted to verify the validity and accuracy of the proposed SFTM. In Section V, a case study is conducted to give more insight into the integration of SFTM into the development and performance evaluation of VICN forwarding schemes. Finally, this paper is concluded in Section VI.

II. RELATED WORK

A. Selective Literature Survey

The networking community has, so far, witnessed the publication of various seminal studies that incorporate traffic models that attempt to emulate realistic vehicular traffic behavior. These traffic models can be classified as follows.

1) *Stochastic Traffic Models*: These models are simplistic and do not account for any of the fundamental principles of the vehicular traffic theory. They describe the random mobility of vehicles using graphs that represent roadway topologies. The movement of vehicles is random, because either individual or a group of vehicles navigate at random speeds over any arbitrary one of the paths represented by the graph. The interactive behavior among vehicles and the correlation between the vehicular density, vehicles' speeds, and the overall traffic flow rate is often neglected or oversimplified. The performance of these models is traditionally contrasted to fully random mobility models that impose no constraints on the nodes' mobility (e.g., random walk [22] and random waypoint [23]). Most stochastic models deviate from reality due to their highly restrictive assumptions.

Examples of stochastic traffic models include the city section mobility model (CSMM), which was introduced in [24]. Under CSMM, all edges of the roadway topology graph are considered bidirectional and 1-D roads. All the edges intersect and form a grid. Vehicles select at random one of the intersections as their travel destination. They move toward this destination at constant speed. Motions are either vertical or horizontal. In addition, the model distinguishes between two speed levels, respectively, a high and a low speed.

In [25], the effect of different mobility models on a selection of vehicular networking performance metrics is investigated. For this purpose, they adopt a freeway mobility model (FMM) and a Manhattan mobility model (MMM). Under FMM, freeways are considered multilane and bidirectional. Furthermore, the vehicular mobility is subject to the following set of constraints: 1) A vehicle is not allowed to switch lanes; 2) the speeds of vehicles are assumed to be uniformly distributed over a specific range; and 3) vehicles must be spaced out by a minimum safety distance. Finally, the authors conduct their study under the assumption that no more than one vehicle exists on the considered roadway segment.

2) *Traffic Stream Models*: Such models interpret vehicular mobility as a hydrodynamic spatiotemporal phenomenon. They

fall under the category of macroscopic models. This is particularly true because they regard vehicular traffic as a flow and relate the following three fundamental macroscopic parameters: 1) the vehicular density; 2) the vehicles' speed; and 3) the traffic flow rate. Traffic stream models do not independently consider the per-vehicle behavior. Instead, they describe the collective behavior of large vehicles streams. This approach renders them of particular utility for high-level analytical studies of traffic behavior as part of the design of data delivery schemes for vehicular networks. Nevertheless, the existing macroscopic models in the open literature are based on different restrictive and case-specific assumptions. Hence, comparing the performance of designed data delivery strategies built on top of these models becomes not meaningful. The networking research community lacks a universal macroscopic model that is simple, realistically accounts for the fundamental principles of vehicular traffic theory and, hence, constitutes the primary building block in the design of vehicular networking data delivery schemes.

The simplest model of this kind was proposed in [20], where the authors assume that the velocity is a function of density. This model can particularly model kinematic waves and has been used over the last couple of years by researchers in vehicular networking.

The work in [26] addresses the joint connectivity and delay-control problem in the context of a highly restrictive macroscopic vehicular mobility model where vehicles navigate at only two speed levels, respectively, high speed V_H and low speed V_L . Precisely, the authors assume that a vehicle may assume a speed level V_H (V_L) for an exponentially distributed amount of time before switching to V_L (V_H) independent of the traffic flow and density, the values of which seemed to arbitrarily be chosen.

In [27], the authors exploit intervehicular communication to establish continuous end-to-end connectivity. However, throughout their study, the authors propose to approximate the macroscopic vehicular traffic dynamics using the combination of the following three approaches: 1) a fluid model; 2) a stochastic model; and 3) a density-dependent velocity profile. Although their proposed approach is remarkably accurate, it is highly complex.

In [28], the Markov decision process (MDP) approach is adopted in their design of a data delivery scheme that has the objective of minimizing the transit delay. In addition to the remarkable complexity of their MDP framework, the authors neglect the correlation between the vehicular flow and speed. Moreover, they assume that vehicle speeds and interarrival times are drawn from known but unspecified probability distributions. These assumptions render their work highly theoretical with limited practicality.

3) *Car-Following Models*: Such models describe the individual behavior of each vehicle relative to a vehicle ahead. Car-following models (for example, see [29]) fall under the category of microscopic models, which are the most commonly employed to analytically delineate vehicular traffic dynamics. In the majority of car-following models, a vehicle's speed and/or acceleration is expressed as a function of factors such as the distance to a front vehicle and the actual speeds of both

vehicles. As such, these models implicitly account for the finite driver's reaction time.

Car-following models are very flexible. They may account for a large number of parameters that pertain, for example, to vehicle technicalities, commuters' skills and habits, and weather constraints, resulting in a remarkable increase of their degree of accuracy and their level of realism. Furthermore, car-following models incorporate lane-changing routines that allow for the regulation of vehicles' mobility in between lanes. Consequently, these models can easily describe the vehicular traffic behavior over individual multilane roadways. Car-following models may also be used to simulate traffic dynamics on independent roadways of an urban scenario. However, in simulations, the interactions between traffic flows at road junctions must be handled with care. In other words, intersections that cross rules in the presence of stop/priority signs and traffic lights have to be defined within the simulation framework. Defining such rules within analytical frameworks is highly complex and often infeasible. This case is particularly true, because the joint complex description of the acceleration of different vehicles, lane changing, and intersection management result in mathematically intractable problems [30]. Compared with macroscopic models, microscopic models, in general, and car-following models, in particular, are characterized by a high level of precision. However, they are highly computationally expensive, particularly whenever the number of simulated vehicles becomes large. It is observed that, in practice, car-following models are avoided when large-scale simulations are conducted. Instead, discrete time models similar to the approach adopted in this paper are employed. Detailed discussions and comparisons on the implementation of different car-following models may be found in [19], [31], and [32].

A concise summary of the aforementioned traffic model categories, together with their advantages and disadvantages, are laid out in Table I.

B. Novel Contributions

Enlightened by rudimentary principles borrowed from the vehicular traffic theory [35], the first contribution of this paper appears in the layout of a concise yet comprehensive study of the free-flow traffic behavior. Precisely, this paper captures the macroscopic vehicular traffic features as described by traffic theorists and characterizes the random density-dependent behavior of traffic flow, vehicle speeds, and travel times using appropriate and highly accurate probability distributions.

Following the macroscopic vehicular traffic study, the second contribution of this paper manifests itself in the foundation of a highly accurate queuing-theory-inspired SFTM. In particular, it is observed that, under free-flow traffic conditions, the probability that a given road segment attains full capacity⁵ is zero. Hence, such a road segment may be modeled as an infinite-server queuing system, and each vehicle that navigates over that segment may be modeled as a job that occupies one of the

⁵One segment of a road has a well-determined length. Consequently, only a finite number of vehicles may simultaneously navigate within that segment. This number is referred to as the capacity of the road segment.

TABLE I
ADVANTAGES AND DISADVANTAGES OF EXISTING TRAFFIC MODELS

Traffic Model Category	Advantages	Disadvantages
Stochastic Traffic Models (e.g. [24], [25])	- Very simplistic and easily tractable.	- Overlook the fundamental principles of vehicular traffic theory. - Neglect the correlation between speed, flow and density.
Traffic Stream Models (e.g. [26]–[28])	- Describe the collective behaviour of large vehicle streams. - Relate the three macroscopic traffic parameters: speed, flow and density. - Useful for high-level analytical studies of traffic behaviour.	- Some of these models (e.g. [26], [28]) are based on unrealistic and case specific assumptions. - Other models (e.g. [27]) are highly complex.
Car Following Models (e.g. [29], [30])	- Account for individual vehicle behaviour relatively to a vehicle ahead. - Analytically delineate vehicular traffic dynamics. - Flexible and account for a large number of parameters.	- Remarkably complex. - Computational power and resource exhaustive. - May easily become analytically intractable (e.g. [30]).

available servers for a finite amount of time. This amount of time is equivalent to the vehicle's residence time (i.e., the amount of time that this vehicle will take to travel the entire segment's length) and depends on the vehicle's speed and the length of the segment. Note that the computation of the mean vehicle's residence time using the proposed vehicle speed distribution, inspired by the vehicular traffic theory, is a complex task. This is particularly true, because these distributions lead to integral expressions that have no closed-form solutions. To work around this problem, we propose to approximate this distribution using a two-phase Coxian distribution, and we show that the proposed approximation leads to highly accurate results. In addition, we characterize one of the major performance measures of this model, which is the instantaneous number of vehicles that reside within the considered road segment. This is equivalent to the instantaneous number of busy servers. In addition, the steady-state distribution of the number of busy servers is determined.

Finally, a case study is presented, with the objective of demonstrating how the proposed SFTM prepares the ground for an adequate design of vehicular networking data delivery schemes. Under free-flow traffic conditions, the vehicular network becomes highly prone to link disruptions. This type of vehicular networks is referred to as a VICN. In the case study presented, we borrow a two-hop VICN scenario based on [28] and [40], where connectivity will be established between the following two isolated SRUs: 1) a source S and 2) a destination D . In the absence of any kind of networking infrastructure, vehicles that pass by S will transport its data bundles to D . For this purpose, a bulk bundle release scheme (BBRS) is built on top of the proposed SFTM. Rigorous mathematical analysis and extensive simulations are conducted to highlight the impact of the underlying traffic model on the performance analysis of data delivery schemes such as BBRS.

III. VEHICULAR TRAFFIC ANALYSIS

A. Free-Flow Traffic Characteristics

Consider a roadway segment $[AB]$ such as the roadway segment depicted in Fig. 1. $[AB]$ has a length L_{AB} (in meters). Let l_v be the mean vehicle length. The *capacity* of $[AB]$ is defined

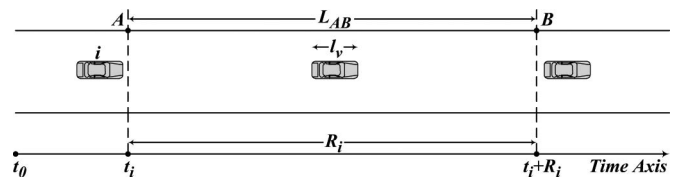


Fig. 1. Free-flow vehicular traffic over the roadway segment $[AB]$.

as $C_{AB} = (L_{AB}/l_v)$ (vehicles) [35]. The mean *vehicular density* ρ_v (in vehicles per meter) is defined as the mean number of vehicles per unit length. Thus, the maximum vehicular density is $\rho_{max} = (C_{AB}/L_{AB}) = (1/l_v)$. The *vehicular flow rate* μ_v (in vehicles per second) is defined as the mean number of vehicles that pass a fixed point on $[AB]$ per unit time.⁶ Without loss of generality, this fixed point is assumed to be the entry point to the segment (i.e., point A). In the following discussion, the event of a vehicle entering $[AB]$ at point A is referred to as a *vehicle arrival*. Therefore, μ_v is interpreted as the *vehicle arrival rate* whose maximum is denoted by μ_{max} . Let S_{max} denote the speed limit over the segment $[AB]$.

The observation of $[AB]$ begins at a certain point in time t_0 (e.g., very early morning) set as the origin of the time axis (i.e., $t_0 = 0$), where $[AB]$ is empty (i.e., no vehicles navigate over $[AB]$, $\rho_v = 0$, and $\mu_v = 0$). After some time, vehicles start arriving to $[AB]$, causing ρ_v to gradually increase with time. μ_v also exhibits a gradual stable⁷ increase as a function of ρ_v . However, there exists a critical density value ρ_c in which, once reached, vehicle platoons start forming all over the road segment $[AB]$. This indicates that $[AB]$ has become considerably congested and the vehicular flow has attained its maximum μ_{max} . At this point, $[AB]$ becomes highly unstable (see [35]), because the slightest traffic perturbation may either restabilize the traffic flow or cause a transition into a state of overforced flow, where μ_v starts decreasing, whereas ρ_v further increases. Eventually, at ρ_{max} , $\mu_v = 0$, indicating that $[AB]$ experiences a traffic jam.

From the point of view of vehicular ad hoc networks (VANETs), the formation of an end-to-end path between an arbitrary pair of nodes becomes highly probable whenever the

⁶In this paper, time is measured in units of *seconds*.

⁷The flow of vehicles into and out of $[AB]$ are equal.

vehicular density is high (i.e., $\rho_c \leq \rho_v \leq \rho_{max}$), regardless of whether those nodes are fixed (e.g., SRUs) or move along the road segment (i.e., vehicles that are equipped with wireless devices). In this situation, delay tolerance is no longer a requirement, and typical wireless protocols can be used over intervehicular-enabled VANETs to establish a multihop connectivity between a particular data source and destination. Obviously, this is not the case whenever the road segment operates under free-flow traffic conditions (i.e., $0 < \rho_v < \rho_c$), where the network becomes sparse and prone to link disruptions. Therefore, cases of overforced vehicular traffic are ignored in this paper.

As shown in Fig. 1, an arbitrary vehicle i with speed s_i enters $[AB]$ at time t_i , resides within $[AB]$ for a period $R_i = (L_{AB}/s_i)$, and exits at time $e_i = t_i + R_i$. Subsequently, vehicle $i + 1$ with speed s_{i+1} arrives at time t_{i+1} , resides within $[AB]$ for a period R_{i+1} , and departs at time e_{i+1} . In the traffic theory, the *time headway* is defined as the time interval between successive vehicles that cross the same reference point on a road segment [35]. In this paper, it is assumed that the reference point is the entry point to $[AB]$ (i.e., point A). Thus, the time headway becomes equivalent to the vehicle interarrival time, which is denoted by $I = t_{i+1} - t_i$. Selecting a distribution for I is a delicate task that has to carefully be handled.

In [15], the authors have conducted thorough experiments over highways surrounding the city of Madrid, Spain. They have collected large sets of realistic traces during the following two separate time intervals: 1) rush hours from 8:30 A.M. to 9:00 A.M. and 2) non-rush hours from 11:30 A.M. to 12:00 P.M. After thorough analysis of their collected data sets, the authors found that I is best modeled by a weighted exponential–Gaussian distribution mixture. Indeed, this finding is of notable importance. In fact, this model particularly accounts for the intervehicular behavioral dependencies under dense traffic conditions and, furthermore, correctly characterizes I , irrespective of the time of the day during which an arbitrary roadway segment is observed. Nevertheless, the primary objective of this paper is the development of a simple macroscopic model to characterize the vehicular traffic behavior under strict free-flow conditions. For this purpose, we need to only consider non-rush hours, i.e., late night and early morning hours from 7:00 P.M. to 8:00 A.M. and midday hours from 10:00 A.M. to 4:00 P.M. The authors in [18] and [33] have also conducted real-life experiments during these hours on the $I - 80$ freeway in California. The realistic data traces that they have obtained show that the vehicle interarrival time during non-rush hours is exponentially distributed. In addition, the analysis presented in [18] shows that, during these hours, particularly whenever the vehicular flow is below 1000 vehicles/h, the intervehicular distance is relatively large. In other words, vehicles that navigate on a roadway segment appear to be isolated, and hence, the vehicle arrivals to an arbitrary geographical reference point become independent and identically distributed. This result has also been confirmed in [15].

Inspired by this last observation, we have conducted thorough simulations using the Simulation for Urban Mobility (SUMO) simulator. SUMO is a microscopic simulator that

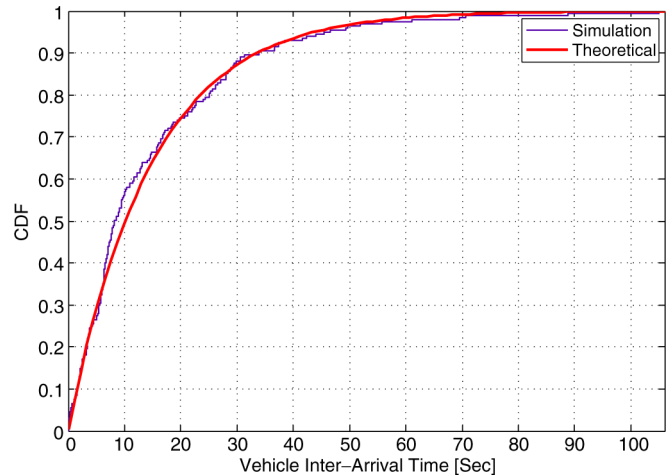


Fig. 2. Vehicle interarrival time cumulative distribution function for a flow rate of 260 vehicles/h.

provides realistic vehicular mobility traces for use as input for other vehicular networking simulators. The same scenario was simulated for different vehicular flow intensities, all of which, however, are less than 1000 vehicles/h. A well-defined geographical reference point was defined for all these simulations, and vehicle arrival times to this reference point were computed. The difference between two consecutive vehicle arrival times gives one sample of the vehicle interarrival time. The conducted simulations spanned a period of time that is long enough to collect 10^5 interarrival time samples per simulation. Due to space limitations, the results of only one simulation scenario are reported herein in Fig. 2. This figure plots the cumulative distribution function of the collected data samples together with its theoretical counterpart. It is, indeed, a tangible proof that I is exponentially distributed.

Note that the mean vehicle interarrival time, $\bar{I} = E[I]$, is inversely proportional to the vehicle arrival rate μ_v . It follows that the probability density function (pdf) of I can be expressed as

$$f_i(t) = \frac{1}{\mu_v} e^{-\frac{t}{\mu_v}} \text{ for } t \geq 0. \quad (1)$$

Denote by \bar{S} the mean of vehicle speeds observed over $[AB]$. It is established in [35] that

$$\bar{S} = S_{max} \left(1 - \frac{\rho_v}{\rho_{max}} \right). \quad (2)$$

Define $\bar{R} = (L_{AB}/\bar{S})$ as the mean vehicle residence time within $[AB]$ and \bar{N} as the mean number of vehicles in $[AB]$. Hence, the following relationship is established using *Little's law*:

$$\mu_v = \frac{\bar{N}}{\bar{R}} = \frac{\bar{N} \cdot \bar{S}}{L_{AB}} = \rho_v \cdot \bar{S} = -\frac{S_{max}}{\rho_{max}} \rho_v^2 + S_{max} \rho_v. \quad (3)$$

According to (3), it is clear that $\mu_v = 0$ at both $\rho_v = 0$ and $\rho_v = \rho_{max}$. In addition, the maximum flow rate $\mu_{max} = (S_{max} \rho_{max}/4)$ occurs at the critical density value $\rho_v = (\rho_{max}/2) = \rho_c$. The critical speed is defined as $S_c = \bar{S}|_{\rho_v=\rho_c} = (S_{max}/2)$. Recall that this paper considers only free-flow traffic conditions (i.e., $\rho_v \in [0; (\rho_{max}/2)]$). According

to [35], under free-flow traffic conditions, the speed s_i ($i > 0$) of an arbitrary arriving vehicle i is a normally distributed random variable with a pdf given by

$$f_S(s_i) = \frac{1}{\sigma_S \sqrt{2\pi}} e^{-\left(\frac{s_i - \bar{S}}{\sigma_S \sqrt{2}}\right)^2}. \quad (4)$$

In [34], it is justifiably assumed that $\sigma_S = k\bar{S}$ and $s_i \in [S_{min}; S_{max}]$, where $S_{min} = \bar{S} - m\sigma_S$, and the two-tuple (k, m) depends on the ongoing traffic activity over the observed roadway segment and is determined based on experimental data. Accordingly, in the rest of this paper, a truncated version of $f_S(s_i)$ in (4) will be adopted. It is defined as

$$\begin{aligned} \widehat{f}_S(s_i) &= \frac{f_S(s_i)}{\int_{S_{min}}^{S_{max}} f_S(s_i) ds_i} \\ &= \frac{2f_S(s_i)}{\operatorname{erf}\left(\frac{S_{max} - \bar{S}_v}{\sigma_{S_v} \sqrt{2}}\right) - \operatorname{erf}\left(\frac{S_{min} - \bar{S}_v}{\sigma_{S_v} \sqrt{2}}\right)} \end{aligned} \quad (5)$$

for $S_{min} \leq s_i \leq S_{max}$. Furthermore, a seminal study that was conducted in [36] together with extensive real-life experimentations and data acquisition over numerous roadways show that s_i is constantly maintained during the vehicle's entire navigation period on the road. Let $\widehat{F}_S(v)$ and $F_R(\tau)$ denote the respective cumulative distribution functions of the vehicle's speed and residence time. It can easily be shown that

$$F_R(\tau) = 1 - \widehat{F}_S\left(\frac{L_{AB}}{\tau}\right) = 1 - \frac{K}{2} \left[1 + \operatorname{erf}\left(\frac{\frac{L_{AB}}{\tau} - \bar{S}}{\sigma_S \sqrt{2}}\right) \right] \quad (6)$$

where $K = 2[\operatorname{erf}(((S_{max} - \bar{S}_v)/\sigma_{S_v} \sqrt{2}) - \operatorname{erf}(((S_{min} - \bar{S}_v)/\sigma_{S_v} \sqrt{2})))]^{-1}$.

Hence, the vehicle's residence time has a pdf that is expressed as

$$f_R(r) = \frac{K \cdot L_{AB}}{r^2 \sigma_S \sqrt{2\pi}} e^{-\left(\frac{\frac{L_{AB}}{r} - \bar{S}}{\sigma_S \sqrt{2}}\right)^2}, r \in \left[\frac{L_{AB}}{S_{max}}; \frac{L_{AB}}{S_{min}}\right]. \quad (7)$$

B. SFTM

Under free-flow traffic conditions, the road segment $[AB]$ experiences low to medium vehicle arrival rates (based on (3), $0 \leq \mu_v \leq \mu_{max}$), whereas the observed vehicle speeds are high (based on (2), $S_c \leq \bar{S} \leq S_{max}$) [34]–[36]. Hence, the probability that $[AB]$ attains full capacity under such conditions is zero. In light of the aforementioned conditions, $[AB]$ can be modeled as an $M/G/\infty$ queuing system, where: 1) Vehicle arrivals follow a Poisson process with parameter μ_v ; 2) the number of busy servers at time t is identical to the number of vehicles within $[AB]$ at time t , which is denoted by $N(t)$; and 3) the busy period of an arbitrary server i is equivalent to the residence time of vehicle i within $[AB]$, whose pdf is given in (7). $N(t)$ is one of the major characteristic measures of this system.

Theorem 3.1: The number of vehicles within $[AB]$ is Poisson distributed with a parameter $\mu_v \bar{R}$.

Proof: Define the following.

- $P_n(t) = \Pr[N(t) = n]$.
- $A_j(t) = \Pr[j \text{ vehicles that arrived in } (0, t)] = ((\mu_v t)^j e^{-\mu_v t} / j!)$.
- $P_{n|j}(t) = \Pr[N(t) = n | j \text{ arrivals in } (0, t)]$.

Therefore

$$P_n(t) = \sum_{j=0}^{\infty} P_{n|j}(t) \cdot A_j(t). \quad (8)$$

The probability that an arbitrary vehicle i that arrived at time t_i is found within $[AB]$ at time t is $1 - F_R(t - t_i)$. Recall that vehicle arrivals follow a Poisson process. Hence, the distribution of the vehicle arrival times conditioned by j arrivals during time interval $(0, t)$ is identical to the uniform distribution of j points over $(0, t)$. Accordingly, the probability that any of the j vehicles that arrived in $(0, t)$ is found within $[AB]$ at time t is given by

$$q(t) = \int_0^t [1 - F_R(t - t_i)] \frac{dt_i}{t} = \frac{1}{t} \int_0^t [1 - F_R(t_i)] dt_i. \quad (9)$$

Consequently, the probability that a vehicle that arrived to $[AB]$ during the time interval $(0, t)$ would have departed from $[AB]$ at time t is

$$1 - q(t) = \frac{1}{t} \int_0^t F_R(t_i) dt_i. \quad (10)$$

Knowing $q(t)$, it is easy to show that

$$P_{n|j}(t) = \begin{cases} \binom{j}{n} [q(t)]^n [1 - q(t)]^{j-n}, & n \leq j \\ 0, & n > j. \end{cases} \quad (11)$$

Using (11), (8) can be rewritten as

$$\begin{aligned} P_n(t) &= \sum_{j=n}^{\infty} \binom{j}{n} [q(t)]^n [1 - q(t)]^{j-n} \cdot \frac{(\mu_v t)^j e^{-\mu_v t}}{j!} \\ &= \frac{[\mu_v t \cdot q(t)]^n e^{-\mu_v t \cdot q(t)}}{n!}. \end{aligned} \quad (12)$$

Note that $\lim_{t \rightarrow \infty} [t \cdot q(t)] = \bar{R}$. Let $N = \lim_{t \rightarrow \infty} N(t)$. Thus, the limiting probability of having $N = n$ vehicles within $[AB]$ is

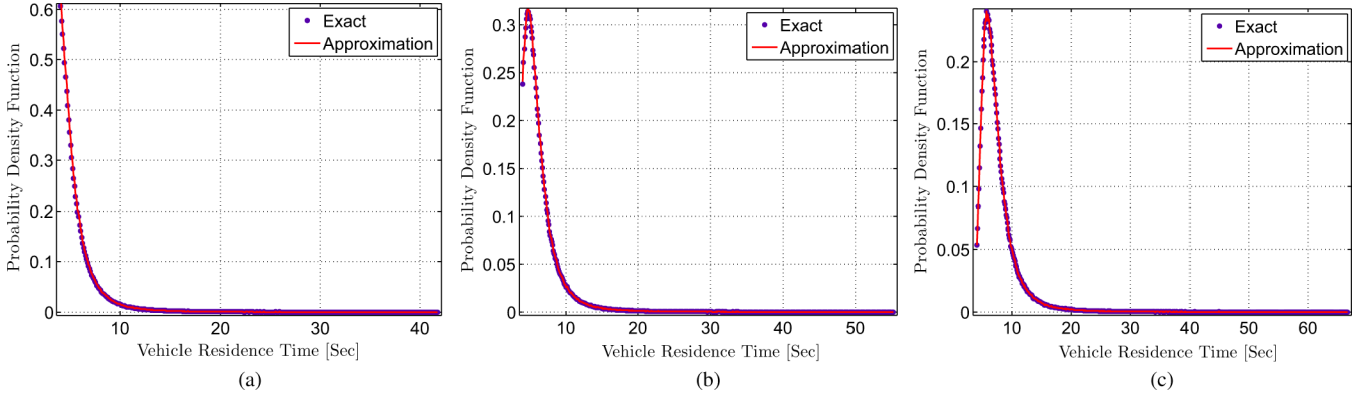
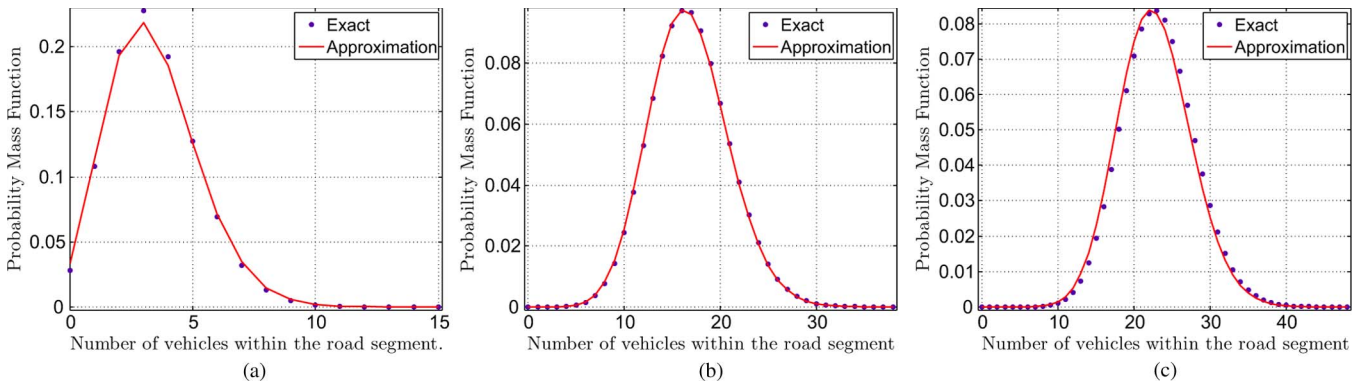
$$P_n = \lim_{t \rightarrow \infty} [P_n(t)] = \frac{(\mu_v \bar{R})^n e^{-\mu_v \bar{R}}}{n!}. \quad (13)$$

Remark: P_n is independent of $f_R(r)$. ■

TABLE II
 MAIN SFTM PARAMETERS

Symbol	Description
L_{AB}	Length of segment $[AB]$
l_v	Mean vehicle length
C_{AB}	Capacity of segment $[AB]$
$\rho_v, \rho_c, \rho_{max}$	Mean, critical and maximum vehicular densities over $[AB]$
μ_v, μ_c, μ_{max}	Mean, critical and maximum vehicular flow rates over $[AB]$
S_{min}, S_{max}, S_c	Minimum, maximum and critical speeds over $[AB]$
$s_i, f_S(s_i), F_S(v)$	Speed of vehicle i , a truncated version of its density and cumulative distribution functions
t_i, e_i	Arrival and departure times of vehicle i
$R_i, f_R(r), F_R(\tau)$	Vehicle residence time, its density and cumulative distribution functions
$I, \bar{I}, f_I(t)$	Inter-arrival time to $[AB]$, its mean and density function
S, \bar{R}, \bar{N}	Mean speed, residence time and number of vehicles within $[AB]$
$N(t), P_n(t), P_{n j}(t)$	Instantaneous number of vehicles within $[AB]$, its density and conditional density functions
$N, P_n, \bar{N}, \bar{P}_n$	Limiting values of $N(t)$ and $P_n(t)$ as $t \rightarrow \infty$ and their approximated versions
$A_j(t)$	Probability of j vehicle arrivals within the interval $(0, t)$
$q(t)$	Probability that any of the j vehicles that arrived in $(0, t)$ is found within $[AB]$ at time t
$\sigma_R^2, \mu_R^2, c_v^2$	Variance, squared mean and squared coefficient of variation of the vehicle residence time
$f_R^{Cox}(r)$	Coxian approximation of $f_R(r)$
\bar{R}	Approximated version of \bar{R}

End of TABLE II


 Fig. 3. $f_R(r)$ versus $f_R^{Cox}(r)$ for different values of ρ_v . (a) $\rho_v = 0.01$. (b) $\rho_v = 0.07$ vehicle/m. (c) $\rho_v = 0.1$.

 Fig. 4. P_n versus \bar{P}_n for different values of ρ_v . (a) $\rho_v = 0.01$. (b) $\rho_v = 0.07$ vehicle/m. (c) $\rho_v = 0.1$.

 At this stage, recall that the pdf of R is given in (7). Thus

$$\bar{R} = \int_0^{\infty} r \cdot f_R(r) dr = \int_0^{\infty} \frac{K \cdot L_{AB}}{r \sigma_S \sqrt{2\pi}} e^{-\left(\frac{L_{AB} - \bar{S}}{r \sigma_S \sqrt{2\pi}}\right)^2} dr. \quad (14)$$

 The complex integral in (14) has no closed-form solution. The squared coefficient of variation $c_v^2 = (\sigma_R^2 / \mu_R^2)$ captures the

 degree of variability of R , where σ_R^2 is the variance of R , and μ_R^2 is the square of its mean. Simple numerical analysis shows that $c_v^2 > 1$. Hence, following the recommendation in [39], $f_R(r)$ may be approximated by a two-phase Coxian density function $f_R^{Cox}(r)$ that is given by

$$f_R^{Cox}(r) = m_1 \cdot \mu_1 e^{-\mu_1 r} + (1 - m_1) \cdot \mu_2 e^{-\mu_2 r} \quad (15)$$

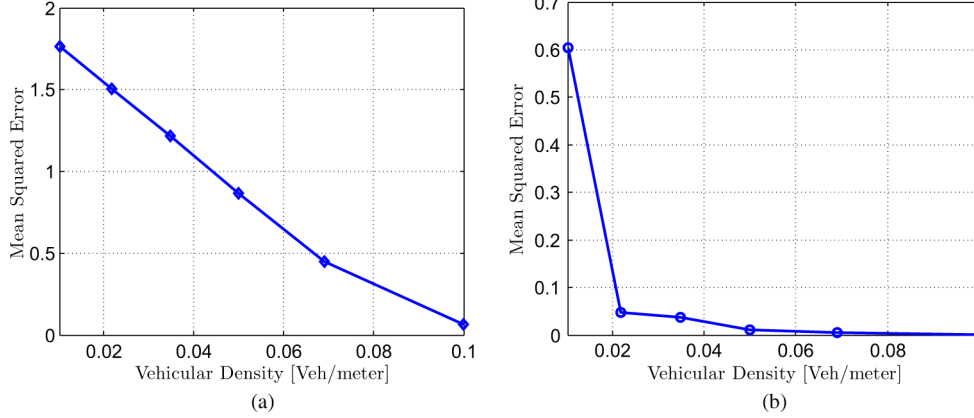


Fig. 5. MSEs (in percentage) for $0.01 \leq \rho_v \leq 0.1$. (a) R . (b) N .

where $\mu_1 = 2\mu_R$, $\mu_2 = (\mu_1/c_v^2)$, and $m_1 = 1 + (\mu_1/2c_v^2(\mu_1 - \mu_2))$. Let \tilde{R} denote an approximated version of R that is computed as

$$\tilde{R} = \int_0^{\infty} r \cdot f_R^{Cox}(r) dr = \frac{m_1}{\mu_1} + \frac{1 - m_1}{\mu_2}. \quad (16)$$

It follows that an approximated version of P_n in (13) is denoted by \tilde{P}_n and is expressed as

$$\tilde{P}_n = \frac{(\mu_v \tilde{R})^n e^{-\mu_v \tilde{R}}}{n!} \quad (17)$$

where \bar{R} is substituted by \tilde{R} . In addition, let \tilde{N} represent the approximated version of \bar{N} . Hence

$$\tilde{N} = \sum_{n=0}^{\infty} n \cdot \tilde{P}_n = \mu_v \tilde{R}. \quad (18)$$

IV. NUMERICAL ANALYSIS AND SIMULATIONS

A Java-based discrete-event simulator was developed to examine the validity and accuracy of the proposed SFTM. The model's characterizing metrics were evaluated for a total of 10^7 vehicles and averaged over multiple simulator runs to ensure the realization of a 95% confidence interval. The following input parameter values were assumed (see Table II): 1) $\rho_v \in [0.005; 0.1]$; 2) $L_{AB} = 200$; and 3) $(k, m) = (0.3, 3)$.

Fig. 3(a) and (c) plots $f_R(r)$ together with $f_R^{Cox}(r)$, as given, respectively, in (7) and (15). Similarly, Fig. 4(a) and (c) plots P_n , as given in (13), concurrent with its approximated counterpart \tilde{P}_n . The accuracy of $f_R^{Cox}(r)$ and of \tilde{P}_n was, respectively, tested for all values of the vehicular density in the range $[0.005, 0.1]$. Results that correspond to $\rho_v = 0.01$, $\rho_v = 0.07$, and $\rho_v = 0.1$ are shown. These results constitute tangible proofs of the validity and high accuracy of the established approximations. This is particularly true, because Fig. 5(a) shows that the highest mean square error (MSE) that results from the approximation of $f_R(r)$ by $f_R^{Cox}(r)$ is 1.67%, and Fig. 5(b) shows that the largest MSE that results from the approximation of P_n by \tilde{P}_n is 0.6%. Finally, extensive simulations were conducted to evaluate

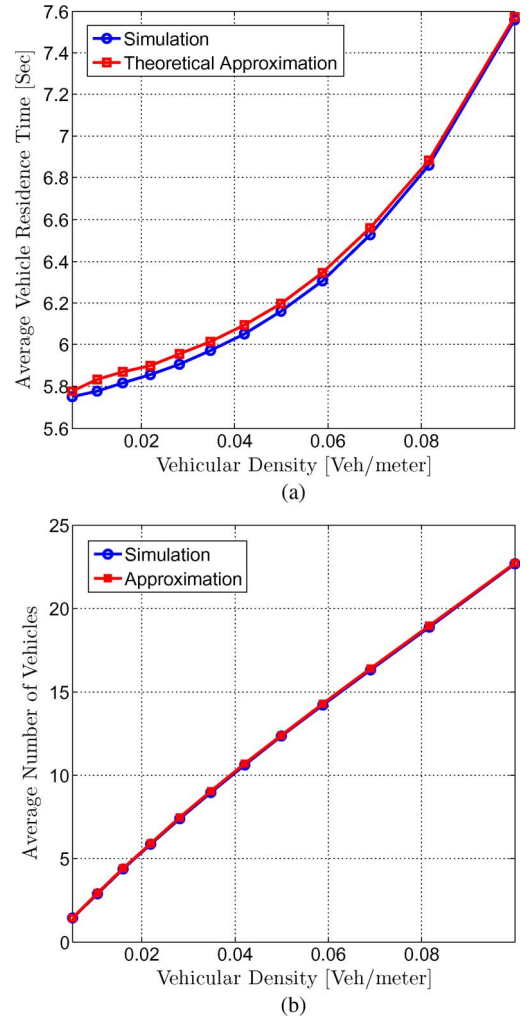


Fig. 6. Variations of R and N as a function of ρ_v . (a) \bar{R} and \tilde{R} versus ρ_v . (b) \bar{N} and \tilde{N} versus ρ_v .

SFTM's characteristics in terms of the mean vehicle residence time and the mean number of vehicles within the road segment. Fig. 6(a) and (b) shows an increase of the mean vehicle's residence time and the mean number of vehicles within $[AB]$ as a function of ρ_v . This case is explained as follows. As ρ_v increases, the mean vehicle speed decreases. Concurrently, the flow of vehicles increases. As a result, $[AB]$ will experience

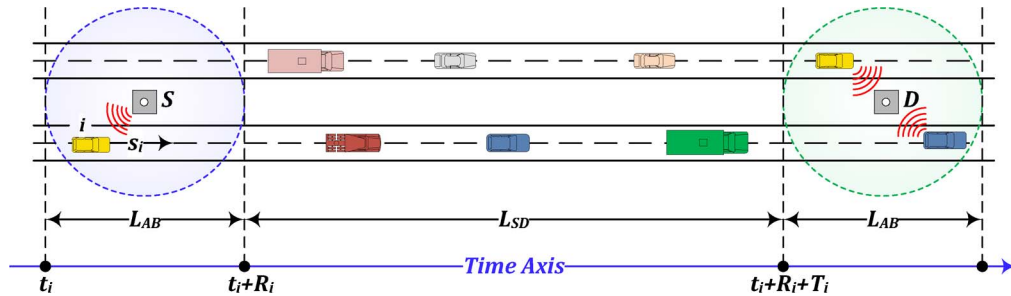


Fig. 7. TH-VICN scenario.

faster vehicle arrivals, and the arriving vehicles will spend more time within $[AB]$.

V. CASE STUDY

This section presents a practical example where the SFTM may be applied.

A. Networking Scenario

Consider the scenario illustrated in Fig. 7, which depicts an uninterrupted highway along which two isolated SRUs, a source S and a destination D , are deployed.⁸ Both S and D have a communication range that covers a segment of the road of length L_{AB} . Moreover, these two SRUs are separated by a distance $L_{SD} \gg L_{AB}$. Connectivity will be established between S and D . In the absence of all sorts of networking infrastructure, wireless nodes that are mounted over mobile vehicles serve as opportunistic *store-carry-forward* devices that transport bundles⁹ from S to D . Vehicles have random speeds and enter the coverage range of S at random time instants. No intervehicle communications may occur. Under such conditions, an intermittence-free end-to-end S - D path does not exist. A network of this type belongs to a subclass of vehicular networks that is conveniently referred to as *two-hop vehicular intermittently connected networks* (TH-VICNs).

B. Motivation

Major wireless operators in the U.S. (e.g., AT&T and Verizon) have recently reported substantial data traffic growth in their networks, which is only partly driven by the utilization of smartphones (e.g., iPhone and BlackBerry). According to Cisco, wireless networks in North America carried approximately 17 PB per month in 2009. It is projected that, in 2014, these networks will carry around 740 PB, i.e., a 40-fold increase. This traffic growth is due to the increased adoption of Internet-connected mobile computing devices and increased data consumption per device. The aggregate impact of these devices on demand for wireless broadband access and the load that they will incur on the service provider networks (SPNs) are expected to be enormous. Despite the recent advancements in

⁸Isolated SRUs are located outside their respective coverage ranges and, therefore, cannot directly communicate.

⁹Data and control signals are combined in a single atomic entity, called bundle, that is transmitted across a DTN [40].

wireless communication technologies, the improvement of both the capacity and coverage of wireless networks has been the limiting factor for unleashing the wireless broadband capabilities. Motivated by the work in [39], we target the exploitation of mobile vehicles as a means of boosting the capacity of legacy wireless networks and extending their coverage ranges. Given their intrinsic tendency to grow to irregular large scales, vehicular networks present unparalleled opportunistic connectivity solutions that contribute to satisfying the exponentially growing user demands for *all-time-anywhere* connectivity, irrespective of the spatiotemporal limitations, as well as offloading data traffic and relieving SPNs from congestions.

The TH-VICN in Fig. 7 becomes of particular utility in rural or other sparsely populated areas where the setup of a wired networking infrastructure may be highly expensive [7]. In these scenarios, SRUs (also known as information relay stations or data posts) are deployed near disconnected sites, and low-cost opportunistic end-to-end connectivity is established through vehicles that ply between these SRUs. Note that very few of these SRUs, called *gateways*, may be connected to the Internet through minimal infrastructure. All other SRUs are completely isolated (even with no direct connectivity) and powered by batteries or small solar cells.¹⁰ Data traffic is then aggregated at source SRUs and appropriately routed through vehicles to destination SRUs. Hence, here, the SRUs can act as both routers or wireless access points in hot spots.

In other scenarios, two sites may be connected through microwave links that may suffer from data traffic overload and from the loss of connectivity due to humidity, rain, storm, clouds, mist, and fog. Hence, deploying SRUs and exploiting the vehicular infrastructure to forward traffic from one site to the other will not only significantly contribute to reducing the load on the microwaves but also provide a protection channel upon their failure under bad atmospheric conditions.

C. Primary Objective

The open literature encloses several proposals of bundle release schemes that aim at achieving delay-minimal bundle delivery in the context of the aforementioned TH-VICN scenario [28], [40]. Although these schemes are particularly appealing, their corresponding analytical performance evaluations are of reduced accuracy, because they are based on restrictive traffic

¹⁰Energy consumption is important in this case but is outside the scope of this paper.

models. In fact, the authors in [28] assume a general distribution of vehicle speeds and do not account for the correlation between the aforementioned macroscopic traffic parameters. In [40], the authors assume uniformly distributed vehicle speeds. This assumption only holds in particular cases of very light traffic. Under such conditions, vehicles may independently navigate at arbitrarily high speeds.

The primary objective of this case study is to give more insight into how the SFTM may be used to evaluate the performance of release schemes such as the approaches proposed in [28] and [40]. In particular, it is of interest to determine the mean bundle end-to-end delay, which is denoted by $\overline{E_d}$ and defined as the mean time that it takes for an arriving bundle at the source SRU S to be delivered to the destination SRU D . Observe that $\overline{E_d}$ is composed of the following two factors: 1) the mean bundle queuing delay $\overline{Q_d}$, defined as the mean time period that a bundle spends in S 's buffer and 2) the mean bundle transit delay $\overline{T_d}$, defined as the mean time that a bundle spends in the buffer of its carrying vehicle until it is delivered to D .

D. Basic Assumptions

For the purpose of this case study, we have the following assumptions.

- A1: The bundle arrivals at the source SRU follow a Poisson process with parameter λ bundles per second.
- A2: All bundles have a fixed size of S_b B.
- A3: The source SRU's transmission rate is T_R b/s.
- A4: The source SRU has an infinite queue size.

Note that assumptions A1–A4 are extracted from [28] and [40], where they have rigorously been justified.

E. Adopted Bundle Release Scheme

The advancements in wireless technology have allowed for data transmission rates on the order of tens of megabits per second, resulting in a negligible bundle transmission time compared to the vehicle residence time.¹¹ Therefore, it becomes more efficient to release as many bundles as possible during the entire vehicle residence time instead of releasing only a single bundle per vehicle. Therefore, for this case study, BBRS is adopted. Under BBRS, the source SRU S uniformly selects one of the vehicles present within its communication range and continuously releases bundles to that vehicle until it goes out of range. Consequently, every vehicle that leaves the coverage range of S will carry a bulk of bundles to be delivered to D . In the following section, a bulk of bundles will simply be referred to as a bulk. The size of a bulk is a random variable that highly depends on the number of buffered bundles at the source and the bundle admission capabilities of the selected vehicle.

F. Modeling and Analysis of BBRS

1) *Vehicle Residence Time*: In this paper, the essence of DTN is preserved. This is particularly true, because it is es-

tablished that the source SRU S has no *a priori* knowledge of vehicle arrival times and speeds. However, similar to [28] and [40], it is assumed that S is equipped with sensors that enable the determination of the speeds of arriving vehicles only at the time of their arrival. Hence, upon the arrival of a vehicle i at time t_i , S determines its speed s_i and residence time $R_i = (L_{AB}/s_i)$. Recall from (5) that $S_{min} \leq s_i \leq S_{max}$. Hence, the maximum and minimum residence times are, respectively, $R_{max} = (L_{AB}/S_{min})$ and $R_{min} = (L_{AB}/S_{max})$. R_i has an approximated pdf $f_R^{Cox}(r)$ as expressed in (15).

2) *Bundle Admission Capability of a Selected Vehicle*: The bundle admission capability of a vehicle i is defined as the maximum number of bundles K_i that a vehicle may receive during its entire residence time R_i . Based on assumptions A2 and A3, the bundle transmission time is $T_b = (8S_b/T_R)$. Therefore, knowing R_i and T_b , the source S computes $K_i = \lfloor (R_i/T_b) \rfloor$. Note that K_i depends on R_i and takes on positive integer values k ($k \in \mathbb{Z}^+$). In addition, it has the respective upper and lower bounds $K_{max} = \lfloor (R_{max}/T_b) \rfloor$ and $K_{min} = \lfloor (R_{min}/T_b) \rfloor$. Hence, the probability mass function of K_i is

$$\begin{aligned} \widetilde{f}_{K_i}(k) &= \int_{kT_b}^{(k+1)T_b} f_R^{Cox}(r) dr = m_1 e^{-\mu_1 k T_b} (1 - e^{-\mu_1 T_b}) \\ &\quad + (1 - m_1) e^{-\mu_2 k T_b} (1 - e^{-\mu_2 T_b}). \end{aligned} \quad (19)$$

It follows that the mean of K_i , which is denoted by \widetilde{K}_i , is computed as

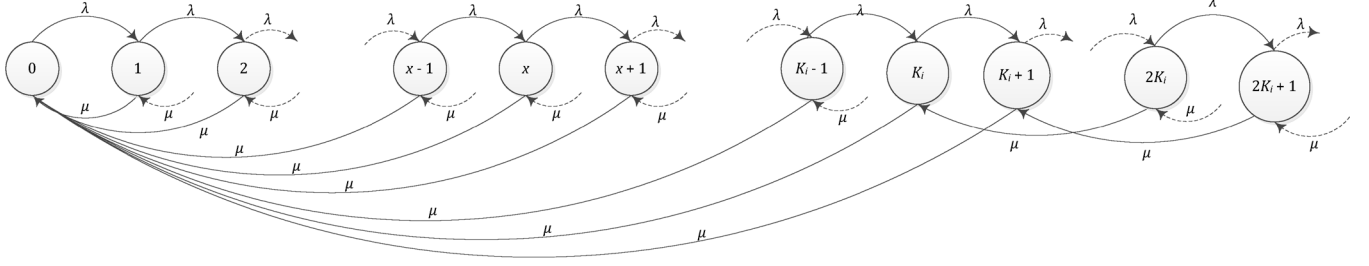
$$\begin{aligned} \widetilde{K}_i &= m_1 (1 - e^{-\mu_1 T_b}) \sum_{k=K_{min}}^{K_{max}} k e^{-\mu_1 k T_b} \\ &\quad + (1 - m_1) (1 - e^{-\mu_2 T_b}) \sum_{k=K_{min}}^{K_{max}} k e^{-\mu_2 k T_b}. \end{aligned} \quad (20)$$

3) *Bulk Size*: The bulk size is a random variable denoted by B_i and depends on both X , representing the number of bundles buffered at S , and K_i . B_i may take on values that depend on the following three identified cases.

- *Case 1*. If $X = 0$, then $B_i = 0$.
- *Case 2*. If $0 < X \leq K_i$, then $B_i = X$.
- *Case 3*. If $X > K_i$, then $B_i = K_i$.

The aforementioned three cases imply the following. For a known value of K_i , bundles are buffered at S and up to K_i of them, if they exist, might be released. Consequently, if $X < K_i$, then all of the X bundles will be released, leaving behind an empty queue. Otherwise, if $X \geq K_i$, only K_i of them are released. Once S completes the transmission of these K_i bundles to vehicle i (which has now departed), it will select a new vehicle, if available, and start handling the remaining bundles in its queue. If no vehicles are readily available, then all remaining bundles will be held in S 's buffer until a vehicle arrives, and so forth. Ultimately, S cannot release more than K_{max} bundles. This only occurs whenever $X \geq K_{max}$ but the arriving vehicle's speed $s_i = S_{min}$. To this end, a source that operates under BBRS can be represented by an $M/M/1$ queuing system with bulk bundle release. It is therefore of

¹¹In this section, the vehicle residence time is defined as the amount of time a vehicle spends in the range of the source SRU.


 Fig. 8. State-transition-rate diagram that represents the behavior of S under BBRs.

interest to resolve this system in light of the new traffic model in Section III and derive closed-form expressions for \bar{X} , which represents the mean number of bundles in the queue. Then, the mean bundle queuing delay is computed using *Little's law*.

4) *Mean Number of Buffered Bundles*: Taking X as a state variable, the state-transition diagram in Fig. 8 represents the behavior of the queuing system under study. Let S_x ($x = 0, 1, 2, \dots$) denote the x th state, indicating that $X = x$. Observe that all states, except for S_0 , are entered both from their left-hand neighbor upon the occurrence of a bundle arrival with a mean rate λ and their K_i -th neighbor to the right upon the occurrence of a bulk departure with a mean rate μ . These states are exited upon the occurrence of either an arrival or a departure. However, state S_0 can only be entered from any one of its immediate right K_i neighbors upon a departure and exited upon an arrival. At this point, it is important to note that μ is a function of the vehicle flow rate μ_v , i.e., the probability that there are no vehicles within the coverage range of the source \tilde{P}_0 and \tilde{K}_i . In fact, after completing the transmission of the most recently released bulk and with a probability \tilde{P}_0 , S will find no available vehicles within its coverage range. Therefore, it will have to wait for the occurrence of the next vehicle arrival to start releasing the next bulk. In this case, the bulk departure rate is $\tilde{P}_0\mu_v$. In contrast, with a probability $1 - \tilde{P}_0$, after completing the transmission of the most recent bulk, S will readily find other vehicles within its coverage range. Hence, it will immediately select one of them, compute its bundle admission capability, and start releasing the corresponding bulk. Under such conditions, the bulk departure rate becomes $((1 - \tilde{P}_0)/\tilde{K}_i T_b)$. It follows that the overall bulk departure rate can be expressed as

$$\mu = \tilde{P}_0\mu_v + (1 - \tilde{P}_0) \frac{1}{\tilde{K}_i T_b}. \quad (21)$$

Without loss of generality, assume that the choice of S falls on a vehicle i . The bundle admission capability that corresponds to this vehicle is K_i . Knowing K_i , denote by $P_{x|K_i}$ the long-term probability of finding x bundles in the system. Therefore, the diagram shown in Fig. 8 leads to the following set of balance equations:

$$\lambda P_{0|K_i} = \mu \sum_{i=1}^{K_i} P_{i|K_i}, \quad \text{for } x = 0 \quad (22)$$

$$(\lambda + \mu) P_{x|K_i} = \lambda P_{(x-1)|K_i} + \mu P_{(x+K_i)|K_i}, \quad \text{for } x \geq 1. \quad (23)$$

Next, the conditional probability mass function of the number of bundles in the queue¹² is derived.

Theorem 5.1: For a known value of $K_i = k$, the conditional probability mass function of the number of bundles in the queue is given by

$$f_{X|K_i}(x) = \left(1 - \frac{1}{z^*(k)}\right) \left(\frac{1}{z^*(k)}\right)^x, \quad x \geq 0. \quad (24)$$

Proof: Let $\tilde{X}(z|K_i) = \sum_{x=0}^{\infty} z^x P_{x|K_i}$ denote the probability generating function of X , given K_i and $\rho = (\lambda/\mu)$. Using [38] and proper manipulation of (20) and (21), it is shown that

$$\tilde{X}(z|K_i) = \frac{\sum_{x=0}^{K_i-1} (z^x - z^{K_i}) P_{x|K_i}}{\rho z^{K_i+1} - (1 + \rho) z^{K_i} + 1}. \quad (25)$$

It can easily be shown, using *Rouche's theorem*, that the denominator in (25) has $K_i + 1$ zeros, of which exactly one occurs at $z = 1$, exactly $K_i - 1$ are such that $|z| < 1$, and only one that we denote by $z^*(K_i)$ will be such that $|z^*(K_i)| > 1$. In addition, observe that the numerator in (25) is a polynomial in z of degree K_i . One of the roots of this numerator is $z = 1$. Recall one of the fundamental properties of probability generating functions that states that $\tilde{X}(z|K_i)$ is bounded by the region $|z| < 1$. As a result, the remaining $K_i - 1$ zeros of the numerator in (25) must exactly match the $K_i - 1$ zeroes of the denominator for which $|z| < 1$. Consequently, the respective polynomials of degree $K_i - 1$ of the numerator and denominator must be proportional, i.e.,

$$\alpha \frac{\sum_{x=0}^{K_i-1} (z^x - z^{K_i}) P_{x|K_i}}{1 - z} = \frac{\rho z^{K_i+1} - (1 + \rho) z^{K_i} + 1}{(1 - z) \left(1 - \frac{z}{z^*(K_i)}\right)} \quad (26)$$

where α is a proportionality constant. Canceling common factors in the numerator and denominator in (26) leads to

$$\tilde{X}(z|K_i) = \frac{1}{\alpha \left(1 - \frac{z}{z^*(K_i)}\right)}. \quad (27)$$

¹²That is, the probability that $X = x$, given that $K_i = k$. We denote this probability mass function as $f_{X|K_i}(x)$.

At this point, the constant α may be found by setting $\tilde{X}(1|K_i) = 1$. This approach results in having

$$\tilde{X}(z|K_i) = \frac{1 - \frac{1}{z^*(K_i)}}{1 - \frac{z}{z^*(K_i)}}. \quad (28)$$

Inverting (28) leads to the probability mass function of X conditioned by $K_i = k$, i.e.,

$$f_{X|K_i}(x) = \left(1 - \frac{1}{z^*(k)}\right) \left(\frac{1}{z^*(k)}\right)^x, \quad x \geq 0. \quad (29)$$

Recall that $K_i \in [K_{min}; K_{max}]$. Hence, the unconditional probability mass function of X is expressed as

$$f_X(x) = \sum_{k=K_{min}}^{K_{max}} \left[m_1 e^{-\mu_1 k T_b} (1 - e^{-\mu_1 T_b}) + (1 - m_1) e^{-\mu_2 k T_b} (1 - e^{-\mu_2 T_b}) \right] \times \left(1 - \frac{1}{z^*(k)}\right) \left(\frac{1}{z^*(k)}\right)^x, \quad x \geq 0. \quad (30)$$

Accordingly, the mean number of bundles in S 's queue is

$$\tilde{X} = E[X] = \sum_{x=0}^{\infty} x \cdot f_X(x). \quad (31)$$

5) *Mean Bundle Queuing Delay*: Using *Little's law*, the mean bundle queuing delay is

$$\tilde{Q}_d = \frac{\tilde{X}}{\lambda}. \quad (32)$$

6) *Mean Bundle Transit Delay*: The transit delay experienced by a bulk of bundles carried by a vehicle i with speed s_i is $T_i = (L_{SD}/s_i)$. T_i has a pdf that is given by

$$f_{T_i}(t) = \frac{K \cdot L_{SD}}{t^2 \sigma_S \sqrt{2\pi}} e^{-\left(\frac{L_{SD}/t - \bar{S}}{\sigma_S \sqrt{2}}\right)^2}, \quad t \in \left[\frac{L_{SD}}{S_{max}}; \frac{L_{SD}}{S_{min}}\right]. \quad (33)$$

Note that $f_{T_i}(t)$ has exactly the same structure as $f_R(r)$ given in (7), with the only difference that L_{AB} is substituted by L_{SD} . Hence, the approximated density function of T_i is given by

$$f_{T_i}^{Cox}(t) = h_1 \cdot \beta_1 e^{-\beta_1 t} + (1 - h_1) \cdot \beta_2 e^{-\beta_2 t} \quad (34)$$

where $\beta_1 = 2\mu_{T_i}$, $\beta_2 = (\beta_1/c_v^2)$, and $h_1 = 1 + (\beta_1/2c_v^2(\beta_1 - \mu_2))$. Note that $\mu_{T_i} = (L_{SD}/\bar{S})$, where \bar{S} is the mean vehicle speed that was experienced under a given vehicular density ρ_v . In addition, $c_v^2 = (\sigma_{T_i}^2/\mu_{T_i}^2)$ is the squared coefficient of variations, where $\sigma_{T_i}^2$ is the variance of T_i .

Let \tilde{T}_d denote the approximated mean bundle transit delay, which is computed as

$$\tilde{T}_d = \int_0^{\infty} t \cdot f_{T_i}^{Cox}(t) dt = \frac{h_1}{\beta_1} + \frac{1 - h_1}{\beta_2}. \quad (35)$$

7) *Mean Bundle End-to-End Delay*: After computing \tilde{Q}_d and \tilde{T}_d , the final step is to compute the mean bundle end-to-end delay \tilde{E}_d . The mean bundle end-to-end delay is equal to the sum of the mean bundle transit delay and the mean bundle queuing delay. Hence

$$\tilde{E}_d = \tilde{Q}_d + \tilde{T}_d. \quad (36)$$

G. BTM

The first objective of this case study is to show how bundle release schemes for TH-VICNs can be designed in light of the proposed traffic model in Section III. In fact, the aforementioned mathematical modeling of BBRS constitutes a sample of a larger theoretical modeling and analysis framework that pertains to more sophisticated bundle release schemes. In addition, the second objective of this case study is to highlight the impact of the underlying traffic model on the performance of such bundle release schemes. For this purpose, in this section, a benchmark traffic model (BTM) is borrowed from [40]. Under BTM, vehicular speeds are assumed to be uniformly distributed in the range $[S_{min}; S_{max}]$. In addition, the correlation between the macroscopic vehicular traffic parameters (i.e., speed, density, and flow) is neglected. See [40] for more details about BTM. In addition, note that the aforementioned analysis of BBRS can easily be refined to fit with BTM. However, to focus on the main objective of this case study, these refinements are omitted.

H. Simulations and Performance Evaluation

To highlight the impact of traffic models on the performance of bundle release schemes, BBRS, which was adopted in this case study, will be tested using the two traffic models SFTM and BTM. In particular, a discrete-event simulation framework is developed to examine the performance of BBRS-SFTM and BBRS-BTM in the context of the sample TH-VICN shown in Fig. 7. The adopted performance metrics are given as follows: 1) the mean queuing delay; 2) the mean transit delay; and 3) the mean end-to-end delay.

1) *Simulator's Input Parameters Values*: BBRS-SFTM is tested under free-flow traffic conditions that correspond to vehicular density values ρ_v in the range of 0.01–0.07 (in vehicles per meter) and flow rate values μ_v in the range of 0.5–2.5 (in vehicles per second; or, equivalently, a mean vehicle interarrival time $\bar{T} \in [4; 20]$ s). The typical IEEE 802.11 protocol is used for SRU-to-vehicle communication, and vice versa, with a data rate of 1 Mb/s. The source is assumed to have a coverage range $L_{AB} = 200$ m, and the source–destination distance is $L_{SD} = 20000$ m. The bundle arrival rate was taken to be $\lambda = 1$ bundle/s, which ensures a fairly heavy offered data load to the source. The bundle size is assumed to be fixed and equal to the maximum transmission unit (MTU), i.e., 1500 B. Following the guidelines in [34], $k = 0.3$, and $m = 3$. The same settings apply for BBRS-BTM, except that, for BTM, vehicle speeds are uniformly distributed in the range [10, 50] m/s.

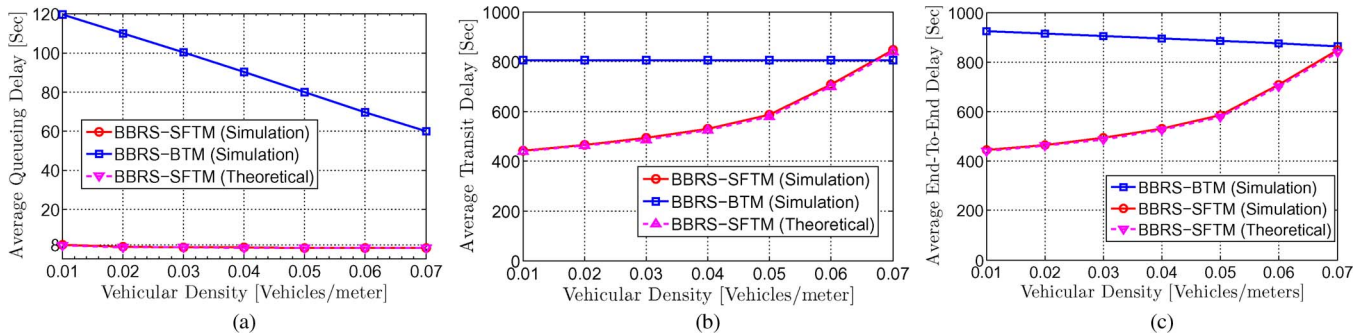


Fig. 9. Performance evaluation of BBRs-SFTM and BBRs-BTM. (a) Mean bundle queuing delay. (b) Mean bundle transit delay. (c) Mean bundle end-to-end delay.

2) *Discussion of Results:* The aforementioned delay metrics were evaluated for a total of 10^7 bundles and averaged over multiple simulator runs to ensure the realization of a 95% confidence interval.

Fig. 9(a)–(c) plots the theoretical mean bundle queuing, transit, and end-to-end delays achieved by BBRs-SFTM concurrent with their corresponding simulated counterparts. Moreover, these figures contrast the different delay performances achieved by BBRs-SFTM to their corresponding performances achieved by BBRs-BTM. These figures constitute tangible proofs of the validity of the proposed mathematical analysis of BBRs based on SFTM and the high accuracy of the established simulation framework.

Fig. 9(a) plots the mean queuing delay achieved by BBRs-SFTM and BBRs-BTM. Both curves are decreasing functions of the vehicular density. In fact, a low vehicular density implies that the vehicular traffic is very light or, alternatively, the vehicle interarrival time is large. Consequently, after completing the transmission of an arbitrary bulk of bundles, the source SRU is less likely to readily find another vehicle within its range. Hence, it will have to wait for the arrival of the next vehicle to proceed to the release of the next bulk. This additional waiting time contributes to the increase of the mean bundle queuing delay. In contrast, as the vehicular density increases, the vehicular traffic flow increases. Thus, the source SRU's busy period tends toward continuity as it becomes more likely to readily find vehicles in range and hence continuously release one bulk after the other. Under such conditions, the mean queuing delay decreases.

Now, notice the impact of the traffic model on the queuing delay performance of BBRs. Although the mean queuing delay that was experienced by bundles under BBRs-SFTM is on the order of a couple of seconds, the mean queuing delay under BBRs-BTM is on the order of tens of seconds. In fact, under BBRs-BTM, vehicle speeds are uniformly distributed within a specific range for all values of the vehicular density. Therefore, a source SRU is equally likely to select a fast or a slow vehicle. Fast vehicles will reside less in the range of the source and have reduced bundle admission capabilities. Consequently, the source SRU will release to those vehicles a mean number of bundles that are smaller than to slow vehicles. Hence, the mean number of accumulating bundles in the queue will increase, and so will the mean queuing delay. In contrast, SFTM reflects the realistic behavior of vehicular traffic where vehicle

speeds decrease as a function of vehicular density. In fact, as the vehicular density increases, the minimum and maximum speeds will decrease and become closer to each other. In other words, it is observed that, as the vehicular density increases, the range of speeds at which vehicles navigate becomes narrower shifts to the left and become more biased toward lower speed values. As a result, vehicles will reside for extended periods of time within the range of the source SRU, where the latter can release remarkably bigger bulks. Consequently, the mean number of queuing bundles will decrease, and so will the mean queuing delay. This case explains the large difference between the queuing delays experienced under BBRs-BTM and BBRs-SFTM.

Fig. 9(b) contrasts the performance of BBRs-SFTM to the performance of BBRs-BTM in terms of the mean transit delay. Because, under BBRs-BTM, vehicle speeds are uniformly distributed over a fixed interval for all vehicular densities, it follows that, irrespective of the vehicular density, the mean speed of bulk transporters is constant and equal to the mean of the chosen interval of speeds. This causes the mean transit delay to become constant for all vehicular densities. However, under BBRs-SFTM, at a low vehicular density, the mean speed of bulk carriers is high. This explains the low mean transit delay. However, the more the vehicular density will increase, the more the speed of transporting vehicles will decrease. Hence, the mean transit delay will increase.

Finally, Fig. 9(c) plots the mean end-to-end delay achieved by BBRs-SFTM and by BBRs-BTM. This goes without saying that the mean end-to-end delay's behavior is clear, because it is the sum of the mean queuing delay and the mean transit delay.

VI. CONCLUSION

This paper has considered a roadway segment $[AB]$ that experiences free-flow vehicular traffic. A comprehensive overview of the macroscopic vehicular traffic dynamics constituted the core of a novel and realistic mathematical framework where an observed roadway segment is modeled using an $M/G/\infty$ queuing system. Closed-form expressions for this model's characteristic parameters were developed. Extensive simulations were conducted to examine the validity and accuracy of the presented model. Finally, a simple case study was presented, with the purpose of providing more insight into the practical application of the proposed model in a real-life

TH-VICN. Note that the model proposed in this paper has a generic fundamental significance that is beyond the specific context of TH-VICNs. Indeed, it can be applied to general systems. Due to this generality, any further results that can be derived have a potential significance for other fields.

REFERENCES

- [1] J. Burgess, B. Gallagher, D. Jensen, and B. N. Levine, "Maxprop: Routing for vehicle-based disruption-tolerant networking," in *Proc. IEEE INFOCOM*, Barcelona, Spain, Apr. 2006, pp. 1–11.
- [2] X. Li, W. Shu, M. Li, H. Huang, and M. Y. Wu, "DTN routing in vehicular sensor networks," in *Proc. IEEE GLOBECOM*, New Orleans, LA, Dec. 2008, pp. 1–5.
- [3] M. Khabzian and M. M. Ali, "A performance modeling of connectivity in vehicular ad hoc networks," *IEEE Trans. Veh. Technol.*, vol. 57, no. 4, pp. 2440–2450, Jul. 2008.
- [4] D. Niyato, P. Wang, and J. C. M. Teo, "Performance analysis of the vehicular delay-tolerant network," in *Proc. IEEE WCNC*, Budapest, Hungary, Apr. 2009, pp. 1–5.
- [5] F. Ye, R. Yim, S. Roy, and J. Zhang, "Efficiency and reliability of one-hop broadcasting in vehicular ad hoc networks," *IEEE J. Sel. Areas Commun.*, vol. 29, no. 1, pp. 151–160, Jan. 2011.
- [6] F. Ye, S. Roy, and H. Wang, "Efficient intervehicle data dissemination," in *Proc. IEEE Veh. Technol. Conf.*, San Francisco, CA, Sep. 2011, pp. 1–5.
- [7] A. Pentland, R. Fletcher, and A. Hasson, "Daknet: Rethinking connectivity in developing nations," *Computer*, vol. 37, no. 1, pp. 78–83, Jan. 2004.
- [8] Fed. Commun. Comm., "Amendment of the Commissions Rules Regarding Dedicated Short-Range Communication Services in the 5.850–5.925 GHz Band," *FCC Rep. & Ord.*, FCC 03-324, 2003.
- [9] *IEEE Draft Standard for Information Technology Telecommunications and Information Exchange Between Systems Local and Metropolitan Area Networks Specific requirements—Part 11: Wireless LAN Medium Access Control (MAC) and Physical Layer (PHY) Specifications, Amendment 7: Wireless Access in Vehicular Environments*, IEEE Std. P802.11pTM/D7.0, May 2009.
- [10] O. K. Tonguz and G. Ferrari, *Ad Hoc Wireless Networks: A Communication-Theoretic Perspective*. Hoboken, NJ: Wiley, 2006.
- [11] N. Wisitpongphan, O. Tonguz, J. Parikh, F. Bai, P. Mudalige, and V. Sadekar, "On the broadcast storm problem in ad hoc wireless networks," in *Proc. Int. Conf. Broadband Commun. Netw. Syst.*, San Jose, CA, Oct. 2006, pp. 1–11.
- [12] M. Torrent-Moreno, D. Jiang, and H. Hartenstein, "Broadcast reception rates and effects of priority access in 802.11-based vehicular ad hoc networks," in *Proc. ACM Int. Workshop VANETs*, Philadelphia, PA, Oct. 2004.
- [13] W. Zhao, M. Ammar, and E. Zegura, "A message ferrying approach for data delivery in sparse mobile ad hoc networks," in *Proc. ACM MobiHoc*, 2004, pp. 187–198.
- [14] K. Fall, "A delay-tolerant network architecture for challenged Internets," Intel Res., Berkeley, CA, Tech. Rep. IRB-TR-03-003, 2003.
- [15] M. Gramaglia, P. Serrano, J. A. Hernandez, M. Calderon, and C. J. Bernardos, "New insights from the analysis of free flow vehicular traffic in highways," in *Proc. IEEE WoWMoM*, Lucca, Italy, Jun. 2011, pp. 1–9.
- [16] R. Baumann, S. Heimlicher, and M. May, "Towards realistic mobility models for vehicular ad hoc networks," in *Proc. IEEE INFOCOM*, Anchorage, AK, May 2007, pp. 73–78.
- [17] J. Yoon, M. Liu, and B. Noble, "Random waypoint considered harmful," in *Proc. IEEE INFOCOM*, San Francisco, CA, Apr. 2003, pp. 1312–1321.
- [18] N. Wisitpongphan, F. Bai, P. Mudalige, V. Sadekar, and O. Tonguz, "Routing in sparse vehicular ad hoc wireless networks," *IEEE J. Sel. Areas Commun.*, vol. 25, no. 8, pp. 1538–1556, Oct. 2007.
- [19] Y. Zhang, "Scalability of car-following and lane-changing models in microscopic traffic simulation systems," M.S. thesis, Louisiana State Univ., Baton Rouge, LA, 2002.
- [20] M. J. Lighthill and G. B. Whitham, "On kinematic waves—Part II: A theory of traffic flow on long crowded roads," in *Proc. Roy. Soc. London A: Math. Phys. Sci.*, 1955, vol. 229, no. 1178, pp. 317–345.
- [21] S. A. Kulkarni and G. R. Rao, "Vehicular ad hoc network mobility models applied for reinforcement learning routing algorithm," in *Contemporary Computing*. Berlin, Germany: Springer-Verlag, 2010, pp. 230–240.
- [22] A. Einstein, "Investigations on the theory of the Brownian motion," in *Einstein: Collected Papers*. New York: Dover, 1926, pp. 170–182.
- [23] D. B. Johnson, D. A. Maltz, and J. Broch, "DSR: The dynamic source routing protocol for multihop wireless ad hoc networks," in *Ad Hoc Networking*. Reading, MA: Addison-Wesley, 2001, pp. 139–172.
- [24] V. Davies, "Evaluating mobility models within an ad hoc network," M.S. thesis, Colorado School Mines, Golden, CO, 2000.
- [25] F. Bai, N. Sadagopan, and A. Helmy, "The IMPORTANT framework for analyzing the impact of mobility on performance of routing protocols for ad hoc networks," *Elsevier Ad Hoc Netw.*, vol. 1, pp. 383–403, 2003.
- [26] A. Abdrabou and W. Zhuang, "Probabilistic delay control and roadside unit placement for vehicular ad hoc networks with disrupted connectivity," *IEEE J. Sel. Areas Commun.*, vol. 29, no. 1, pp. 129–139, Jan. 2011.
- [27] I. W.-H. Ho, K. K. Leung, and J. W. Polak, "Stochastic model and connectivity dynamics for VANETs in signalized road systems," *IEEE/ACM Trans. Netw.*, vol. 19, no. 1, pp. 195–208, Feb. 2011.
- [28] V. Ramaiyan, E. Altman, and A. Kumar, "Delay optimal schedule for a two-hop vehicular relay network," *Mobile Netw. Appl.*, vol. 15, no. 1, pp. 97–111, May 2009.
- [29] D. C. Gazis, R. Herman, and R. W. Rothery, "Nonlinear follow-the-leader models of traffic flow," *Oper. Res.*, vol. 9, pp. 545–567, 1961.
- [30] *Revised Monograph on Traffic Flow Theory*, Turner-Fairbank Highway Res. Center, McLean, VA, Tech. Rep., 2001.
- [31] S. Panwai and H. Dia, "Comparative evaluation of microscopic car-following behavior," *IEEE Trans. Intell. Transp. Syst.*, vol. 6, no. 3, pp. 314–325, Sep. 2005.
- [32] M. Aycin and R. Benekohal, "Comparison of car-following models for simulation," *Transp. Res. Rec.: J. Transp. Res. Board*, vol. 1678, pp. 116–127, 1999.
- [33] N. Wisitpongphan, F. Bai, P. Mudalige, and O. K. Tonguz, "On the routing problem in disconnected vehicular ad hoc networks," in *Proc. IEEE INFOCOM*, 2007, pp. 2291–2295.
- [34] M. Rudack, M. Meincke, and M. Lott, "On the dynamics of ad hoc networks for intervehicles communications," in *Proc. ICWN*, Las Vegas, NV, Jun. 2002.
- [35] R. P. Roess, E. S. Prassas, and W. R. McShane, *Traffic Engineering*, 3rd ed. Englewood Cliffs, NJ: Prentice-Hall, 2004.
- [36] J. H. Banks, "Freeway speed-flow-concentration relationships: More evidence and interpretations," *Transp. Res. Rec.*, vol. 1225, pp. 53–60, 1989.
- [37] D. R. Cox, "A use of complex probabilities in the theory of stochastic processes," *Math. Proc. Cambridge Philosoph. Soc.*, vol. 51, no. 2, pp. 313–319, Apr. 1955.
- [38] J. F. Hayes and T. V. J. Ganesh Babu, *Modeling and Analysis of Telecommunications Networks*. Hoboken, NJ: Wiley Interscience, 2004, pp. 86–89.
- [39] M. Grossglauser and D. N. C. Tse, "Mobility increases the capacity of ad hoc wireless networks," *IEEE/ACM Trans. Netw.*, vol. 10, no. 4, pp. 477–486, Aug. 2002.
- [40] M. Khabbaz, W. F. Fawaz, and C. M. Assi, "A probabilistic bundle relay strategy in two-hop vehicular delay-tolerant networks," in *Proc. IEEE ICC*, Kyoto, Japan, Jun. 2011, pp. 1–6.



Maurice J. Khabbaz received the B.E. and M.Sc. degrees (with honors) in computer engineering from the Lebanese American University (LAU), Byblos, Lebanon, in 2006 and 2008, respectively. He is currently pursuing the Ph.D. degree in electrical engineering with Concordia University, Montreal, QC, Canada.

Between 2006 and 2008, he served as a Communications and Control Systems Laboratory and Computer Proficiency Course Instructor and a Teaching and Research Assistant of Electrical and Computer Engineering with LAU, where he was appointed as the President of the School of Engineering and Architecture Alumni Chapter Founding Committee and was elected the Executive Vice President of this chapter in 2007. He is currently a full-time Researcher in electrical engineering with Concordia University. His research interests include delay/disruption-tolerant networks, wireless mobile networks, and queuing theory.



Wissam F. Fawaz received the B.E. degree in computer engineering from the Lebanese University, Beirut, Lebanon, in 2001, the M.Sc. degree in network and information technology from the Pierre and Marie Curie University (University of Paris VI), Paris, France, in 2002, and the Ph.D. degree (with excellent distinction) in network and information technology from the University of Paris XIII, in 2005.

Since October 2006, he has been an Assistant Professor of electrical and computer engineering with the Lebanese American University, Byblos, Lebanon. His research interests include next-generation optical networks, survivable network design, and queuing theory.

Dr. Fawaz received the French Ministry of Research and Education Scholarship for Distinguished Students in 2002 and a Fulbright Research Award in 2008.



Chadi M. Assi (SM'08) received the B.Eng. degree from the Lebanese University, Beirut, Lebanon, in 1997 and the Ph.D. degree from the City University of New York (CUNY) in April 2003.

He is currently an Associate Professor with the Concordia Institute for Information Systems Engineering, Concordia University, Montreal, QC, Canada. Before joining Concordia University in August 2003 as an Assistant Professor, he was a Visiting Scientist for one year with Nokia Research Center, Boston, MA, where he worked on quality of service

in passive optical access networks. He is an Associate Editor for *Wiley Wireless Communications and Mobile Computing*. His research interests include optical networks, multihop wireless and ad hoc networks, and security.

Dr. Assi received the prestigious Mina Rees Dissertation Award from CUNY in August 2002 for his research on wavelength-division-multiplexing optical networks. He is on the Editorial Board of the IEEE COMMUNICATIONS SURVEYS AND TUTORIALS and serves as an Associate Editor for the IEEE COMMUNICATIONS LETTERS.